Asymmetric Catalysis

Actuation of Asymmetric Cyclopropanation Catalysts: Reversible Single-Crystal to Single-Crystal Reduction of Metal–Organic Frameworks**

*Joseph M. Falkowski, Cheng Wang, Sophie Liu, and Wenbin Lin**

Over the past decade, metal–organic frameworks (MOFs) have provided an excellent platform for engineering functional materials through judicious choices of the constituent building blocks. Numerous MOFs have been synthesized, and some of them have been explored for potential applications such as gas storage,[1] chemical sensing,[2] catalysis,[3] biomedical imaging,[4] and drug delivery.[5] Catalytic MOFs having imbedded, well-defined active sites are of particular interest owing to their utility as recyclable and reusable catalysts. Because of their highly ordered and typically crystalline structures, MOF catalysts can in principle be characterized by X-ray diffraction methods to provide precise structural information on the catalytic active sites, thus allowing the delineation of catalyst structure–function relationships.[6] Herein we report the first observation of the actuation of a MOF catalyst through a reversible single-crystal to single-crystal reduction process.

Among many strategies for synthesizing catalytic MOFs, direct incorporation of catalytically competent building blocks into the MOF frameworks has recently emerged as a powerful approach toward building highly active and selective solid catalysts.[3,7] Motivated by excellent asymmetric catalytic activities exhibited by many homogeneous metal/salen complexes [where an archetypal chiral salen ligand is (R,R)-1,2-cyclohexanediamino-N,N'-bis(3-*tert*-butyl-salicylidene)],[8] MOFs containing metal/salen building blocks have attracted a great deal of recent interest.[9] Whereas some of the chiral metal/salen-based MOFs have shown promise in chiral recognition and separation,[10] two manganese/salen-derived MOF systems have recently been shown to be excellent asymmetric alkene epoxidation catalysts.[11] In this work, a pair of interpenetrated and non-interpenetrated chiral MOFs (CMOFs) of the primitive cubic unit (pcu) topology were constructed from redox active ruthenium/salen-based bridg-

ing ligands and $[Zn_4(\mu_4\text{-}O)(O_2CR)_6]$ secondary building units (SBUs). These CMOFs showed the first example of reversible single-crystal to single-crystal reduction/reoxidation behavior. Although a few examples of single-crystal to single-crystal oxidation of MOFs were reported, none of these redox reactions were demonstrated to be reversible.[12] In contrast, the reduction of a MOF was recently elucidated by a Rietveld analysis of powder X-ray diffraction data.[13] We report here that upon single-crystal to single-crystal reduction, catalytically inactive Ru^{III}-based CMOFs were activated to form Ru^{II}-based MOF catalysts for the asymmetric cyclopropanation of styrene and other substituted alkenes with very high diastereo- and enantioselectivities (d.r. = 7:1 and *ee* = 91 %). The catalytic activity of the CMOFs is catenation dependent: the non-interpenetrated CMOF is highly active whereas the interpenetrated CMOF is nearly inactive. We also show that the CMOFs maintain their crystallinity, and less than 0.01 % of the ruthenium/salen catalyst leached into the solution after the catalytic reaction.

The enantiopure ruthenium(II) complex, [Ru(**L**-Me$_2$)(py)$_2$] (py = pyridine), where **L**-Me$_2$ is the methyl ester of (R,R)-$(-)$-N,N'-(methyl-3-carboxyl-5-tert-butylsalicylidene)-1,2-cyclohexanediamine, was prepared by a metathesis reaction between the potassium salt of **L**-Me$_2$ and [{RuCl$_2$(p-cymene)}$_2$]. Saponification of [Ru(**L**-Me$_2$)(py)$_2$] and subsequent acidification with dilute hydrochloric acid and air oxidation resulted in the Ru^{III}/salen-derived dicarboxylic acid, [Ru(**L**-H$_2$)(py)$_2$]Cl. The diamagnetic complex [Ru(**L**-Me$_2$)(py)$_2$] was characterized by ^{1}H and ^{13}C NMR spectroscopy, whereas the paramagnetic [Ru(**L**-H$_2$)(py)$_2$]Cl was characterized by MS and single-crystal X-ray diffraction (Figure 1 a).[14]

Solvothermal reactions of [Ru(**L**-H$_2$)(py)$_2$]Cl with Zn-(NO$_3$)$_2$·6H$_2$O in DBF/DEF/EtOH (DBF = dibutylformamide, DEF = N,N-diethylformamide) or in DEF/DMF/EtOH (DMF = N,N-dimethylformamide) at 80 °C afforded, after 36 hours, dark-green, cuboid single crystals of the twofold interpenetrated CMOF **1** with the formula {Zn$_4$(μ_4-O)[(Ru(**L**-H$_2$)(py)$_2$Cl]$_3$}·(DBF)$_7$·(DEF)$_7$, and the non-interpenetrated CMOF **2** with the formula {Zn$_4$(μ_4-O)[(Ru(**L**-H$_2$)(py)$_2$Cl]$_3$}·(DEF)$_{19}$·(DMF)$_5$·(H$_2$O)$_{17}$ (Figure 1 b).[15] Compound **1** crystallizes in the $R32$ space group,[14] with the asymmetric unit containing two [Ru(**L**)(py)$_2$]Cl ligands and two-thirds of a Zn$_4$(μ_4-O) cluster composed of two Zn atoms of full occupancy and two Zn atoms of one-third occupancy, as well as two O atoms of one-third occupancy. As expected, the carboxylate groups from six adjacent [Ru(**L**)(py)$_2$]Cl ligands coordinate to the four Zn centers to form [Zn$_4$(μ_4-

[*] J. M. Falkowski, C. Wang, S. Liu, Prof. W. Lin
Department of Chemistry, CB#3290, University of North Carolina, Chapel Hill, NC 27599 (USA)
E-mail: wlin@unc.edu
Homepage: http://www.chem.unc.edu/people/faculty/linw/wlindex.html

© 2011 Wiley-VCH Verlag GmbH & Co. KGaA, Weinheim

WILEY ONLINE LIBRARY
8833

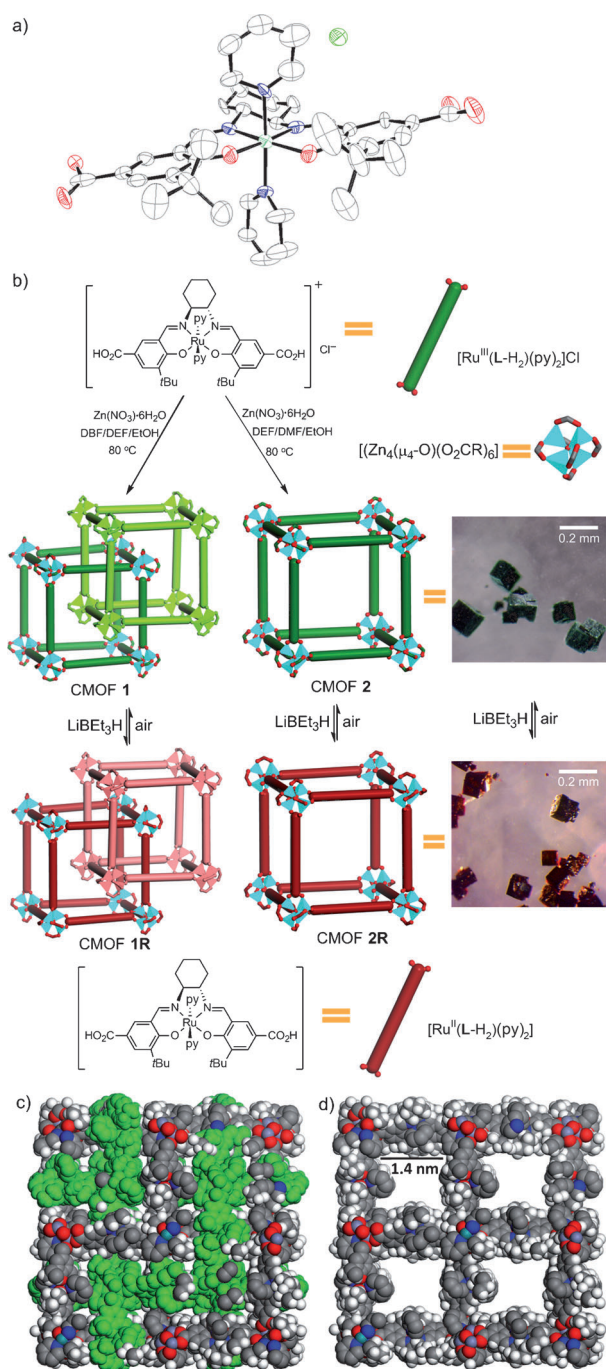**Figure 1.** a) ORTEP drawing of the $[Ru^{III}(L-H_2)(py)_2]Cl$ ligand as determined from single-crystal X-ray diffraction. The thermal ellipsoids are shown at 50% probability. b) Synthesis and single-crystal to single-crystal reduction/oxidation of **1** and **2**. The photographs illustrate the typical colors and morphologies of **2** (green) and **2R** (red). c) Space-filling model of **1** as viewed perpendicular to the (1 0 −2) plane. d) Space-filling model of **2** as viewed perpendicular to the (1 0 −2) plane.

O)(O$_2$CR)$_6$] SBUs, which are linked by the [Ru(**L**)(py)$_2$]Cl ligands to form a three-dimensional network of the pcu topology (Figure 1b). Because of the elongated [Ru(**L**)-(py)$_2$]Cl ligands, **1** adopts a twofold interpenetrated structure with 54.5 % of void space, as calculated by PLATON, that is

filled with the DBF, DEF, and ethanol molecules. The precise solvent content could not be determined by X-ray crystallography owing to its disordered nature. The solvent content was instead established by a combination of ^{1}H NMR studies and thermogravimetric analyses (TGA; see the Supporting Information). The largest cavities in the interpenetrated networks of **1** measure 0.8 nm in diameter and are connected to each other by 0.4×0.3 nm^2 windows (Figure 1c).

Compound **2** crystallizes in the *R3* space group with very similar unit-cell dimensions and the same asymmetric unit content as **1**.[14] The framework of **2** is exactly identical to one of the two interpenetrating nets in **1** having the same metal–ligand connectivity and network topology (Figure 1b). The *R3* space group symmetry of **2**, however, led to a non-interpenetrated structure. As a result, **2** enjoys much larger open channel dimensions of 1.4×1.0 nm^2 and a cavity size of 1.7 nm (Figure 1d), with 78.8 % of void space as calculated by PLATON.

Compounds **1** and **2** can be readily identified on the basis of the differences in their powder X-ray diffraction (PXRD) patterns. As indicated in our previous work on CMOFs made from manganese/salen-derived dicarboxylic acid bridging ligands,[11b] the twofold interpenetrated **1** showed additional systematic absences in the PXRD because of the presence of a pseudo *4$_3$* screw axis (Figure 2a). The structures of **1** and **2** are also supported by their solvent weight losses determined by TGA; **1** and **2** exhibited approximately 40 and 50 wt % solvent loss, respectively, in the 25–200 °C temperature range. We have also recently demonstrated the use of dye inclusion assays in differentiating catenated versus noncatenated MOFs.[11b, 16] Dye-inclusion studies with brilliant blue R-250 indicated a 5 wt % and 30 wt % dye uptake for **1** and **2**,
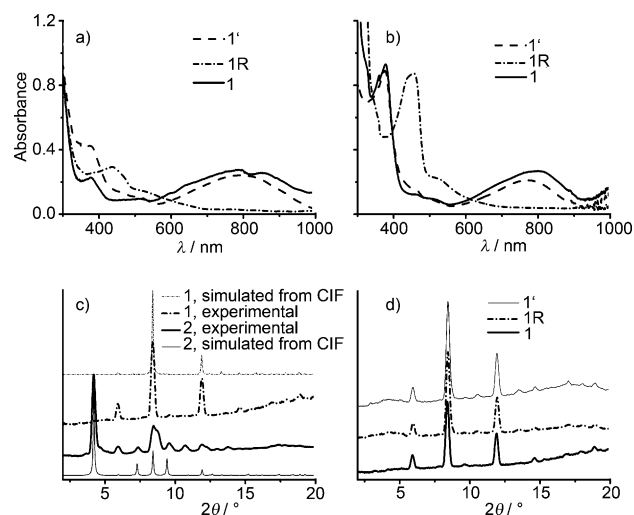

Figure 2. a) Experimental and simulated PXRD patterns of **1** and **2**. The peak at 2θ ca. 4.3°, which corresponds to the Miller indices 1 0 −2, is missing in the PXRD of **1** because of the pseudo *4$_3$* screw axis. b) Diffuse reflectance and c) solution absorption spectra of **1**, **1R**, and **1′**, thus demonstrating reversible reduction of **1** to **1R** with LiBEt$_3$H and reoxidation of **1R** to **1′** in air. The solution spectra were taken by dissolving CMOFs in pyridine. d) PXRD patterns of **1**, **1R**, and **1′**. Their similarity supports the reversible single-crystal to single-crystal reduction of **1** to **1R** and reoxidation of **1R** to **1′**.
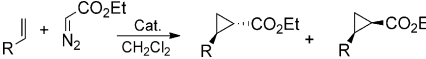
respectively. Similarly, **1** and **2** exhibit an uptake of 0.4 and 12.4 wt % of crystal violet, respectively. These results additionally confirm the different catenation behaviors for **1** and **2**.

Treatment of **1** and **2** with strong reducing agents such as LiBEt$_3$H (superhydride) or NaB(OMe)$_3$H led to a color change from dark green to dark red, thus suggesting the reduction of the Ru^{III} centers to Ru^{II} centers in the CMOFs. The reduced CMOFs, **1R** and **2R**, exhibited very different UV/Vis/NIR diffuse reflectance spectra from those of **1** and **2** (Figure 2b). Upon reduction of **1** and **2**, the characteristic Ru^{III}/salen ligand-to-metal charge-transfer (LMCT) bands at 771 nm disappeared, with concomitant appearance of new peaks at 520 nm that are indicative of the Ru^{II}/salen ^{1}MLCT bands.[17] These results were confirmed by the solution absorption spectra of the corresponding CMOFs dissolved in pyridine (Figure 2c). Interestingly, the reduction of **1** and **2** occurred in a single-crystal to single-crystal fashion. **1R** and **2R** retained their single-crystal nature with the same space groups and similar cell parameters as those of **1** and **2**, respectively. Single-crystal X-ray structure studies additionally indicated that the structures of **1R** and **2R** are essentially identical to those of **1** and **2**, respectively. Even more remarkably, **1R** and **2R** can be re-oxidized in air to afford dark green CMOF crystals of **1′** and **2′**, which is supported by the diffuse reflectance and solution UV/Vis/NIR absorption spectra. Single-crystal to single-crystal reduction/reoxidation processes in **1** and **2** are thus entirely reversible. PXRD and unit-cell determinations indicated that **1′** and **2′** remained single crystals with the same structures as **1** and **2** (Figure 2d and see the Supporting Information). This work represents the first example of totally reversible single-crystal to single-crystal reduction/oxidation processes in MOFs.[8,9]

Nguyen et al. elegantly demonstrated that the [Ru(salen)(py)$_2$] complex is a competent homogeneous cyclopropanation catalyst that transfers the carbene fragment from ethyldiazoacetate to various olefins with excellent enantio- and diastereoselectivities.[18] We hypothesized that the present ruthenium/salen-derived CMOFs could catalyze the cyclopropanation reactions heterogeneously. Using styrene and other substituted alkenes as test substrates, we have evaluated the activity of **1R** and **2R** towards enantio- and diastereoselective cyclopropanation reactions.

After reduction of **2** with LiBEt$_3$H, the resulting **2R** was washed repeatedly with anhydrous THF and then with dichloromethane. The cyclopropanation reaction between styrene and ethyldiazoacetate was carried out in the presence of 3 mol % of **2R** under anaerobic conditions for 24 hours. Disappointingly, the **2R**-catalyzed cyclopropanation reaction afforded the cyclopropane products in less than 8 % yield with a *trans/cis* diastereomeric ratio (d.r.) of 4.2 (Table 1, entry 1). The enantiomeric excesses (*ee*) for the *trans-* and *cis-*cyclopropane products were 65 % and 51 %, respectively. We noticed that the color of the **2R** suspension always turned dark green during the cyclopropanation reactions, and we reasoned that the Ru^{II} centers in **2R** were readily oxidized

Table 1: Asymmetric cyclopropanation of substituted olefins using CMOF catalysts.[a]

Entry	Catalyst	R	Mol% cat.	Yield [%]	d.r.	ee [%] (trans)	ee [%] (cis)
1	**2R**	Ph	3	7.8	4.2	65	51
2	**2R**[b]	Ph	3	54	7	91	84
3	**2**	Ph	3	1	–	–	–
4	**1R**	Ph	3	1	1.2	33	47
5	[Ru(**L**-Me$_2$)(py)$_2$]	Ph	1	28	9.6	92	85
6	[Ru(**L**-Me$_2$)(py)$_2$][b]	Ph	1	53	10.9	98	92
7	**2R**[b]	OEt	2	20	2	61	67
8	[Ru(**L**-Me$_2$)(py)$_2$][b]	OEt	2	37	2.6	77	79
9	**2R**[b]	CH$_3$(CH)$_2$	2	27	1.7	25	13
10	[Ru(**L**-Me$_2$)(py)$_2$][b]	CH$_3$(CH)$_2$	2	47	1.7	29	24
11	Zn-BPDC	Ph	n/a[c]	<1	–	–	–

[a] For reaction conditions see Experimental section. [b] With NaBH(OMe)$_3$ in solution. [c] n/a = not applicable.

and thus deactivated during the cyclopropanation reactions. Consistent with this hypothesis, the control reaction with **2** as the catalyst did not produce any cyclopropane product (Table 1, entry 3). To prevent the **2R** catalyst from oxidizing and deactivating, we carried out the cyclopropanation reaction in the presence of NaBH(OMe)$_3$. A much improved yield (54 %) of cyclopropane products was obtained under these reaction conditions, with a d.r. of 7 in favor of the *trans* products and *ee* values of 91 % and 84 % for the *trans* and *cis* products, respectively (Table 1, entry 2). Interestingly, a similar cyclopropanation reaction with **1R** as the catalyst gave the desired products in less than 1 % yield and with modest *ee* values (Table 1, entry 4). The framework interpenetration in **1R** significantly reduced the open channel sizes, thus preventing the diffusion of the reagents into the Ru^{II}/salen active sites in the interior of **1R**. The beneficial effect of a reducing agent for the cyclopropanation reaction was also observed for the homogeneous control reaction with the [Ru(**L**-Me$_2$)(py)$_2$] catalyst: The cyclopropane products were obtained in a yield of 28 % and 53 % in the absence or presence, respectively, of NaBH(OMe)$_3$ (Table 1, entries 5 and 6). Finally, we have shown that **2R** is also an active catalyst for the cyclopropanation of both 1,3-pentadiene and ethyl vinyl ether, albeit in lower yields and with lower d.r. and *ee* values, as is the case for [Ru(**L**-Me$_2$)(py)$_2$]-catalyzed cyclopropanation reactions (Table 1, entries 7–10).

We have also tested the heterogeneity of the CMOF catalysts. The supernatants from the cyclopropanation reactions after filtration through a 0.45 μm filter did not afford additional cyclopropane products. The CMOF catalysts were recyclable and the recovered CMOF catalysts showed activity in subsequent runs of cyclopropanation reactions, albeit in reduced yields and stereoselectivities (see the Supporting Information). We believe that the reduced yields and stereoselectivities of the recovered CMOFs are a result of the intrinsic instability of the Ru^{II}/salen cyclopropanation catalyst but not the dissolution or decomposition of the CMOFs. Leaching experiments were performed on both **1** and **2**. UV/Vis and ICP-MS analyses indicated that less than

0.01% of the ruthenium was leached into solution after 24 hours under the typical reaction conditions. The CMOF catalysts recovered from the catalytic reaction retained their crystallinity as indicated by the similarity of their PXRD patterns to those of the pristine solids (see Figures S31 and S32 in the Supporting information). Finally, attempts to carry out cyclopropanation reactions with the Zn-BPDC (BPDC = 4,4'-biphenyldicarboxylic acid) MOF[19] did not produce any cyclopropane product, thus confirming the catalytic activity of the $[Ru(\mathbf{L})(py)_2]$ strut in the present studies.

In summary, we have synthesized a pair of interpenetrated and non-interpenetrated CMOFs using a redox active ruthenium/salen-derived dicarboxylate bridging ligands. The as-synthesized Ru^{III}/salen MOFs underwent unprecedented reversible single-crystal to single-crystal reduction/reoxidation. The reduction of the Ru^{III} CMOFs turned on the catalytic activity, and the resulting Ru^{II} CMOFs were highly active for the asymmetric cyclopropanation of substituted alkenes with very high diastereo- and enantioselectivities. This pair of reduced CMOFs also exhibited remarkable catenation-dependent catalytic activity; non-interpenetrated **2R** was highly active whereas interpenetrated **1R** was nearly inactive because of its inability to transport the substrates through its small channels. The CMOF catalyst was recyclable and reusable, with less than 0.01% of the ruthenium/salen catalyst leaching into the solution after the catalytic reaction. We also showed that the CMOFs maintained their crystallinity after the catalytic reaction. This work highlights the ability to structurally interrogate active MOF catalysts, and promises to provide important insights into MOF-catalyzed organic transformations.

Experimental Section

Synthesis of $Zn_4O(\mathbf{L})_3\cdot(DEF)_7\cdot(DBF)_7$ (CMOF-1). 1 mg of $[Ru(\mathbf{L}\text{-}H_2)(py)_2]Cl$ (1.2 µmol) and 1 mg of $Zn(NO_3)_2\cdot6H_2O$ (3.4 µmol) were dissolved in 0.2 mL of DBF and 0.1 mL of DEF in a 0.5 dram screw-capped vial. 20 µL of ethanol was added to this solution, and the vial was heated to 80°C for 1 day to afford green cubes (0.76 mg, 61% yield). Solvent content was calculated from the proposed formula: DMF: 16.0%; DBF: 24.8%; that determined by ^{1}H NMR/TGA studies: DBF: 25.0%; DEF: 16.0%.

Procedure for single-crystal to single-crystal reduction/reoxidation. A sample of the CMOF **2** was washed with ethanol and dry THF. The sample was then treated with an excess of LiBEt$_3$H (1M in THF) and allowed to stand for 5 min, after which the sample was washed with THF. For single-crystal data sets, the crystal was then immersed in chlorobenzene and mounted in a capillary tube. For reoxidation, the reduced crystals were suspended in CH$_2$Cl$_2$ and left to sit in a capped vial overnight.

Asymmetric cyclopropanation reactions with CMOFs. CMOF **2** (7 mg, 4.6 µmol) was washed with ethanol and dry THF and then treated with LiBEt$_3$H. The sample stood for 5 min before being washed with dry THF three more times. The sample was then washed with dry CH$_2$Cl$_2$ and degassed. Styrene (80 µL, 780 µmol) was added to the suspension, and ethyl diazoacetate (EDA; 16.5 µL, 156 µmol) was added dropwise over 30 min. After addition of the EDA, the reaction mixture was stirred for 24 h. The suspension was then passed through a 0.45 µm filter and analyzed by chiral GC.

[1] a) M. Dinca, J. R. Long, *Angew. Chem.* **2008**, *120*, 6870; *Angew. Chem. Int. Ed.* **2008**, *47*, 6766; b) J. L. Rowsell, O. M. Yaghi, *Angew. Chem.* **2005**, *117*, 4748; *Angew. Chem. Int. Ed.* **2005**, *44*, 4670; c) B. Kesanli, Y. Cui, M. R. Smith, E. W. Bittner, B. C. Bockrath, W. Lin, *Angew. Chem.* **2005**, *117*, 74; *Angew. Chem. Int. Ed.* **2005**, *44*, 72; d) W. Yang. A. Greenaway, X. Lin, R. Matsuda, A. J. Blake, C. Wilson, W. Lewis, P. Hubberstey, S. Kitagawa, N. R. Champness, M. Schröder, *J. Am. Chem. Soc.* **2010**, *132*, 14457.

[2] a) M. D. Allendorf, R. J. Houk, L. Andruszkiewicz, A. A. Talin, J. Pikarsky, A. Choudhury, K. A. Gall, P. J. Hesketh, *J. Am. Chem. Soc.* **2008**, *130*, 14404; b) B. Chen, L. Wang, Y. Xiao, F. R. Fronczek, M. Xue, Y. Cui, G. Qian, *Angew. Chem.* **2009**, *121*, 508; *Angew. Chem. Int. Ed.* **2009**, *48*, 500; c) S. Pramanik, C. Zheng, X. Zhang, T. J. Emge, J. Li, *J. Am. Chem. Soc.* **2011**, *133*, 4153–4155; d) Z. Xie, L. Ma, K. E. deKrafft, A. Jin, W. Lin, *J. Am. Chem. Soc.* **2010**, *132*, 922.

[3] a) B. Kesanli, W. Lin, *Coord. Chem. Rev.* **2003**, *246*, 305; b) J. Lee, O. K. Farha, J. Roberts, K. A. Scheidt, S. T. Nguyen, J. T. Hupp, *Chem. Soc. Rev.* **2009**, *38*, 1450; c) L. Ma, C. Abney, W. Lin, *Chem. Soc. Rev.* **2009**, *38*, 1248; d) G. Nickerl, A. Henschel, R. Grunker R, K. Gedrich, S. Kaskel, *Chem. Ing. Tech.* **2011**, *83*, 90.

[4] a) K. E. deKrafft, Z. Xie, G. Cao, S. Tran, L. Ma, O. Z. Zhou, W. Lin, *Angew. Chem.* **2009**, *121*, 10085; *Angew. Chem. Int. Ed.* **2009**, *48*, 9901; b) W. Lin, W. J. Rieter, K. M. Taylor, *Angew. Chem.* **2009**, *121*, 660; *Angew. Chem. Int. Ed.* **2009**, *48*, 650.

[5] a) W. J. Rieter, K. M. Pott, K. M. L. Taylor, W. Lin, *J. Am. Chem. Soc.* **2008**, *130*, 11584; b) P. Horcajada, T. Chalati, C. Serre, B. Gillet, C. Sebrie, T. Baati, J. F. Eubank, D. Heurtaux, P. Clayette, C. Kreuz, J. S. Chang, Y. K. Hwang, V. Marsaud, P. N. Bories, L. Cynober, S. Gil, G. Ferey, P. Couvreur, R. Gref, *Nat. Mater.* **2010**, *9*, 172; c) K. M. L. Taylor-Pashow, J. Della Rocca, Z. Xie, S. Tran, W. Lin, *J. Am. Chem. Soc.* **2009**, *131*, 14261.

[6] L. Ma, C.-D. Wu, M. M. Wanderley, W. Lin, *Angew. Chem.* **2010**, *122*, 8420; *Angew. Chem. Int. Ed.* **2010**, *49*, 8244.

[7] a) A. Hu, H. L. Ngo, W. Lin, *J. Am. Chem. Soc.* **2003**, *125*, 11490; b) A. Hu, H. L. Ngo, W. Lin, *Angew. Chem.* **2003**, *115*, 6182; *Angew. Chem. Int. Ed.* **2003**, *42*, 6000.

[8] a) T. P. Yoon, E. N. Jacobsen, *Science* **2003**, *299*, 1691; b) M. Palucki, N. S. Finney, P. J. Pospisil, M. L. Guler, T. Ishida, E. N. Jacobsen, *J. Am. Chem. Soc.* **1998**, *120*, 948; c) W. Zhang, J. L. Loebach, S. R. Wilson, E. N. Jacobsen, *J. Am. Chem. Soc.* **1990**, *112*, 2801.

[9] a) M. Oh, C. A. Mirkin, *Angew. Chem.* **2006**, *118*, 5618; *Angew. Chem. Int. Ed.* **2006**, *45*, 5492; b) Y. M. Jeon, J. Heo, C. A. Mirkin, *J. Am. Chem. Soc.* **2007**, *129*, 7480; c) S. Jung, M. Oh, *Angew. Chem.* **2008**, *120*, 2079; *Angew. Chem. Int. Ed.* **2008**, *47*, 2049; d) R. Kitaura, G. Onoyama, H. Sakamoto, R. Matsuda, S. Noro, S. Kitagawa, *Angew. Chem.* **2004**, *116*, 2738; *Angew. Chem. Int. Ed.* **2004**, *43*, 2684; e) B. Chen, X. Zhao, A. Putkham, K. Hong, E. B. Lobkovsky, E. J. Hurtado, A. J. Fletcher, K. M. Thomas, *J. Am. Chem. Soc.* **2008**, *130*, 6411.

[10] G. Yuan, C. Zhu, W. Xuan, Y. Cui, *Chemistry* **2009**, *15*, 6428.

[11] a) S.-H. Cho, B. Ma, S. T. Nguyen, J. T. Hupp, T. E. Albrecht-Schmitt, *Chem. Commun.* **2006**, 2563; b) F. Song, C. Wang, J. M. Falkowski, L. Ma, W. Lin, *J. Am. Chem. Soc.* **2010**, *132*, 15390–15398; F. Song, C. Wang, W. Lin, *Chem. Commun.* **2011**, *47*, 5256–8258.

[12] a) H. J. Choi, M. P. Suh, *J. Am. Chem. Soc.* **2004**, *126*, 15844; b) M. P. Suh, Y. E. Cheon, *Aust. J. Chem.* **2006**, *59*, 605; c) Y.-G. Huang, B. Mu, P. M. Schoenecker, C. G. Carson, J. R. Karra, Y.

Cai, K. S. Walton, *Angew. Chem.* **2011**, *123*, 456; *Angew. Chem. Int. Ed.* **2011**, *50*, 436.

[13] M. Meilikhov, K. Yusenko, A. Torrisi, B. Jee, C. Mellot-Draznieks, A. Pöppl, R. A. Fischer, *Angew. Chem.* **2010**, *122*, 6348; *Angew. Chem. Int. Ed.* **2010**, *49*, 6212.

[14] The determination of the unit cell and data collections for crystals of [Ru(**L**-H$_2$)(Py)$_2$]Cl, **1**, **1R**, **2**, and **2R** were performed on a Bruker SMART APEX II diffractometer. Crystallographic data for [Ru(**L**-H$_2$)(Py)$_2$]Cl: Monoclinic, space group *C2*, $a =$ 19.703(1), $b = 25.895(2)$, $c = 18.631(2)$ Å, $\beta = 90.381(4)°$, $V =$ 9505.5(10) Å^3, $Z = 8$, $\rho_{calcd} = 1.321$ g cm^{-3}, $R1(I>2\sigma(I)) = 0.0718$, $wR2(I>2\sigma(I)) = 0.174$. Crystallographic data for **1**: Trigonal, space group *R32*, $a = 29.750$ (2), $c = 72.886(7)$ Å, $V =$ 55865(7) Å^3, $Z = 6$, $\rho_{calcd} = 0.884$ g cm^{-3}, $R1(I>2\sigma(I)) = 0.177$, $wR2(I>2\sigma(I)) = 0.401$. Crystallographic data for **2**: Trigonal, space group *R3*, $a = 29.681$ (1), $c = 72.690(2)$ Å, $V =$ 55457(2) Å^3, $Z = 3$, $\rho_{calcd} = 0.445$ g cm^{-3}, $R1(I>2\sigma(I)) = 0.138$, $wR2(I>2\sigma(I)) = 0.337$. Crystallographic data for **1R**: Trigonal, space group *R32*, $a = 29.798$ (1), $c = 73.027(2)$ Å, $V =$ 56153(2) Å^3, $Z = 6$, $\rho_{calcd} = 0.879$ g cm^{-3}, $R1(I>2\sigma(I)) = 0.163$,

$wR2(I>2\sigma(I)) = 0.376$. Crystallographic data for **2R**: Trigonal, space group *R3*, $a = 29.724$ (1), $c = 72.861(2)$ Å, $V =$ 55750(2) Å^3, $Z = 3$, $\rho_{calcd} = 0.443$ g cm^{-3}, $R1(I>2\sigma(I)) = 0.171$, $wR2(I>2\sigma(I)) = 0.263$. CCDC 816123, 816124, 816125, 816126, and 816127 contain the supplementary crystallographic data for this paper. These data can be obtained free of charge from The Cambridge Crystallographic Data Centre via www.ccdc.cam.ac.uk/data_request/cif.

[15] The solvent-dependent catenation behavior observed here is different from the CMOFs built from manganese/salen struts (see Ref. [11b]) and probably a result of different solubility of the CMOFs in these solvents.

[16] L. Ma, J. M. Falkowski, C. Abney, W. Lin, *Nat. Chem.* **2010**, *2*, 838.

[17] M. Muthukumar, P. Viswanathamurthi, K. Natarajan, *Spectrochim. Acta Part A* **2008**, *70*, 1222.

[18] J. A. Miller, W. Jin, S. T. Nguyen, *Angew. Chem.* **2002**, *114*, 3077; *Angew. Chem. Int. Ed.* **2002**, *41*, 2953.

[19] M. Eddaoudi, J. Kim, N. Rosi, D. Vodak, J. Wachter, M. O'Keeffe, O. M. Yaghi, *Science* **2002**, *295*, 469.